0254-6124/2016/36(5)-805–10 *Chin. J. Space Sci.* 空间科学学报

XIE Wenjun, LUO Xinghong, ZHANG Xingwang, YU Yude. Microgravity Material Research in China: 2016. *Chin. J. Space Sci.*, 2016, **36**(5): 805-814. DOI:10.11728/cjss2016.05.805

Microgravity Material Research in China: 2016

XIE Wenjun[1] LUO Xinghong[2] ZHANG Xingwang[3] YU Yude[3]

1(*North Western Polytechnical University, Xi'an* 710072)

2(*Institute of Metal Research, Chinese Academy of Sciences, Shenyang* 110016)

3(*Institute of Semiconductors, Chinese Academy of Sciences, Beijing* 100083)

Abstract Firstly, recent research works of high undercooling and rapid solidification of metallic alloys under ground simulation conditions in Northwestern Polytechnical University are reviewed. Secondly, under normal gravity and microgravity of binary to quinary Nickel-base single crystal alloys with different contents of W, Ta, Al and Ti elements are comparatively investigated by Institute of Metal Research using drop tube. Thirdly, solidification and crystal growth of SJ10-Recoverable Scientific Experiment Satellite by Institute of Semiconductors is introduced.

Key words Undercooling, Simulation, Crystallization, Microgravity, Superalloys solidification

Classified index V 524

1 High Undercooling and Rapid Solidification of Metallic Alloys under Ground Simulation Conditions

1.1 Space Environment Simulation by Electrostatic and Acoustic Levitation

Electrostatic levitation is an efficient method for the study of undercooling and solidification of high temperature melts under containerless condition. Wei and his coworkers developed an electrostatic levitator based on a systematic optimization of the electric field, position detecting, sample charging and voltage feedback control[1]. Various types of materials such as metals, inorganic materials and polymers were stably levitated (Figure 1)[2]. This apparatus can also levitate various kinds of plant seeds and flower buds such as coral berry, peppers, soybeans, wheat grains and mushroom[3]. Using this levitator, the density and ratio of specific heat to emissivity of Ni_7Zr_2 intermetallic alloy[4] and $Zr_{91.2}Si_{8.8}$ eutectic alloy[5] have been measured, which is found to vary linearly with

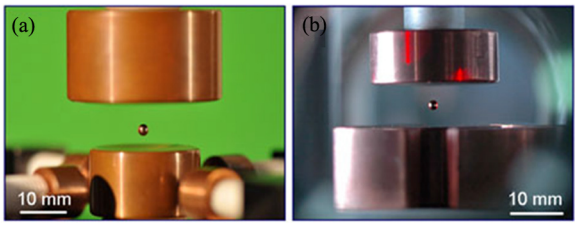

Fig. 1 Electrostatic levitation of metallic materials. (a) Ti-6Al-4V alloy in air, (b) Ir in vacuum

Received May 31, 2016

E-mail: yudeyu@semi.ac.cn

temperature at solid and liquid states. The obtained maximum undercooling of Ni_7Zr_2 and $Zr_{91.2}Si_{8.8}$ alloy melts reaches 317 K and 371 K, respectively. The eutectic growth velocity of $Zr_{91.2}Si_{8.8}$ alloy was measured to be $1\,mm{\cdot}s^{-1}$ for lamellar eutectic and $90\,mm{\cdot}s^{-1}$ for anomalous eutectic.

Acoustic levitation is another practical technique for containerless processing of materials, especially for those with poor conductivity and low melting temperature. In order to improve the stability of single-axis acoustic levitator, Wei and his group carried out a series of optimum design of the reflector[6]. Two kinds of flexible reflectors were proposed. One kind is those with a deformable reflecting surface, and the other kind is those with an elastic support, both of which are self-adaptive to the change of acoustic radiation pressure[6]. With the elastic reflector, the levitation stability can be remarkably enhanced by reducing the decay time and amplitude of the sample vibration[7]. The containerless melting and solidification of several alloys have been successfully achieved by applying the elastically supported reflector and with the assistance of a YAG laser beam. An interesting phenomenon is the appearance of surface wave patterns on the acoustically levitated and solidified eutectic alloy samples[8]. To understand the solidification mechanism under acoustic levitation condition, the fluid dynamics of levitated drops was also extensively studied. In addition to the general vertical vibration and axisymmetric shape oscillation[9], a special kind of non-axisymmetric mode, *i.e.* sectorial oscillation was observed[10]. The sectorial oscillation was excited by parametric resonance and the eigenfrequency can be well described by a modified Rayleigh equation. The internal fluid always flows between the extended sections and the compressed sections [11]. They also discovered a kind of vortex flow rotating in the meridional plane of the steadily levitated drop[12].

1.2 Thermophysical Properties of Undercooled Liquid Multicomponent Alloys

The thermophysical properties of undercooled metallic melts are difficult to measure because of the severe requirements for experimental conditions. Appling the electromagnetic levitation techniques and incorporating the oscillating drop method and drop calorimetry method, Wei and his coworkers have measured the surface tension and specific heat of a series of undercooled liquid alloys in Ti-Al binary system[13−14], Ti-Al-Nb ternary system[15−16] and Ni-based multicomponent systems[17−18]. For Ti-Al system, the maximum undercoolings of $Ti_{80}Al_{20}$, $Ti_{55}Al_{45}$, $Ti_{49}Al_{51}$ alloys are obtained to be 257 K ($0.13\,T_L$), 259 K ($0.143\,T_L$), 324 K ($0.19\,T_L$), respectively (see Figure 2). Their surface tension varies linearly with temperature in the experimental range. The specific heat of liquid $Ti_{80}Al_{20}$ and $Ti_{49}Al_{51}$ alloys are determined to be 33.01 and $31.27\,J{\cdot}mol{\cdot}K^{-1}$

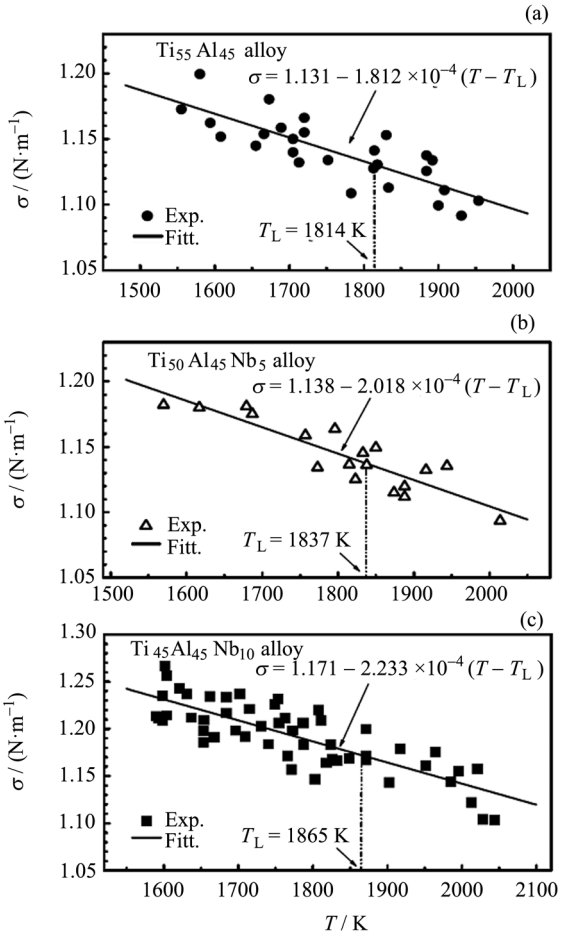

Fig. 2 Surface tension of liquid Ti-Al and Ti-Al-Nb alloys versus temperature. (a) $Ti_{55}Al_{45}$ alloy, (b) $Ti_{50}Al_{45}Nb_5$ alloy, and (c) $Ti_{45}Al_{45}Nb_{10}$ alloy

in the superheated and undercooled states. For Ti-Al-Nb system, the maximum undercoolings of $Ti_{50}Al_{45}Nb_5$ and $Ti_{45}Al_{45}Nb_{10}$ alloys are 268 K ($0.146\,T_L$) and 287 K ($0.15\,T_L$), respectively. The specific heat of liquid $Ti_{45}Al_{45}Nb_{10}$ alloy is determined to be $32.72\,J{\cdot}mol{\cdot}K^{-1}$ over a broad temperature range of 1578—2010 K. The surface tension of Ti-Al-Ni alloys decreases linearly with the increase of temperature. For Ni-based multicomponent alloys, the maximum undercoolings of $Ni_{90}Cu_5Fe_5$, $Ni_{80}Cu_{10}Fe_{10}$, $Ni_{85}Cu_5Fe_5Sn_5$, $Ni_{80}Cu_5Fe_5Sn_5Ge_5$, and $Ni_{75}Cu_5Fe_5Co_5Sn_5Ge_5$alloys are 272 K ($0.15\,T_L$), 252 K ($0.15\,T_L$), 349 K ($0.21\,T_L$), 363 K ($0.22\,T_L$), and 363 K ($0.22\,T_L$), respectively. The specific heats of $Ni_{80}Cu_{10}Fe_{10}$ and $Ni_{75}Cu_5Fe_5Co_5Sn_5Ge_5$ alloys are measured to be 41.67 and $41.49\,J{\cdot}mol{\cdot}K^{-1}$, respectively. The surface tension of $Ni_{90}Cu_5Fe_5$, $Ni_{85}Cu_5Fe_5Sn_5$, and $Ni_{80}Cu_5Fe_5Sn_5Ge_5$ alloys are determined as 1.799, 1.546 and $1.357\,N{\cdot}m^{-1}$ at their liquidus temperatures, and with their temperature coefficients to be -4.972×10^{-4}, -5.057×10^{-4}, and $-5.385\times10^{-4}\,N{\cdot}m^{-1}{\cdot}K^{-1}$, respectively. Based on these directly measured values, other thermophysical parameters such as viscosity and diffusion coefficient can also be derived. Computer simulation is an efficient way to investigate the structure and thermodynamical properties of undercooled liquid metals and alloys at atomic scale. Wei and coworkers carried out an extensive Molecular Dynamics (MD) simulation on the structures and thermophysical properties of undercooled liquid Ni, Fe, Cu, Co, Ti, Pd, Pt, Ag, Au and Rh pure metals[19], and Fe-Cu binary[20] and Ni-Cu-Fe ternary[21] systems. The densities, specific heats, and atomic order parameters were obtained and analyzed for these metals and alloys by MD simulation, and some results were compared with the measured data or existing theories, which shows reasonable consistency. As a complementary study, the structure, elastic and thermodynamic properties of crystalline alloys and compounds were conducted by a First-principle calculation[22]. Differential Scanning Calorimetry (DSC) and laser flash method were also employed to determine the enthalpy of fusion, undercoolibility and thermal diffusivity of the multicomponent alloys [23].

1.3 Rapid Solidification Kinetics and New Materials Development

Dendrites and eutectics are the two elementary growth patterns in solidification. Rapid dendritic growth kinetics of undercooled liquid alloys was quantitatively studied by Wei and coworkers with the help of electromagnetic levitation and glass fluxing methods. The dendrite growth velocities of γ-Fe, α-Ni, and Ni_3Sn phases were measured in undercooled Fe-based and Ni-based alloys. Generally, the growth velocity varies with the increase of undercooling according to a power or exponential law. The measured maximum velocities of γ-Fe dendrite attains 15 and $30.4\,m{\cdot}s^{-1}$ in $Fe_{50}Cu_{50}$[24] and $Fe_{62.5}Cu_{27.5}Sn_{10}$[25] alloys, respectively. The dendritic growth velocity of undercooled pure Fe was also determined as a reference, which reaches $69\,m{\cdot}s^{-1}$[24]. The growth velocity of α-Ni phase in undercooled liquid $Ni_{90}Cu_5Mo_5$[26] and $Ni_{85}Cu_5Mo_5Ge_5$[27] alloys approached 32 and $28\,m{\cdot}s^{-1}$, respectively. The Ni_3Sn compound grows dendritically like a solid solution phase with a nonfaceted manner in $Ni_{66}Sn_{31.7}Ge_{2.5}$ alloy[28] and the maximum velocity was measured to be only $0.38\,m{\cdot}s^{-1}$. At high undercoolings, a morphological transition usually takes place from well-developed dendrites to equiaxed grains, and the rapid growth velocity leads to a significant solute trapping. Rapid eutectic growth in Ni-Sn[29], Al-Ge[30], and Al-Cu-Si[31] systems was investigated under acoustic levitation and free fall conditions. It was found that a lamellar eutectic to anomalous eutectic transition usually takes place if the undercooling is large enough.

Peritectic and monotectic solidification processes are sensitive to undercooling and often exhibits immiscibility, which is a great challenge for the fabrication of homogeneously dispersed materials. Wei and his group performed extensive exploration on the undercooling, phase separation and microstructural

characterization of these two kinds of solidification by means of drop tube, glass fluxing, and acoustic levitation. Peritectic phase forms *via* peritectic transformations in most cases. Once the undercooling exceeds a critical value, the peritectic phase grows directly from the undercooled liquid by suppressing the primary phase nucleation and peritectic transformation. This has been demonstrated experimentally in Cu-Sn system[32]. The ternary Fe-Cu-Sn[25], Fe-Cu-Si[33], and Co-Cu-Ni[34] alloys possess a metastable immiscibility gap. If the alloy melts were undercooled into this gap, liquid phase separation is possible to become the dominant solidification mechanism, and a morphological transition from dendrites to macrosegregation was observed in the solidified microstructures. During the free fall of Fe-Sn-Si[35], Fe-Sn-Ge (see Figure 3)[36] and Co-Cu-Pb[37] ternary alloy droplets, core-shell structures of two or three layers were frequently formed after solidification owing to the liquid phase separation and the reduced gravity. But for sufficiently small droplets, the macrosegregation can be suppressed so as to form a homogeneously dispersed microstructure. The phase separation of Al-Cu-Sn alloy[38] under acoustic levitation condition shows a laterally-layered macro-segregation which is much special as compared to the vertically-layered pattern under normal condition.

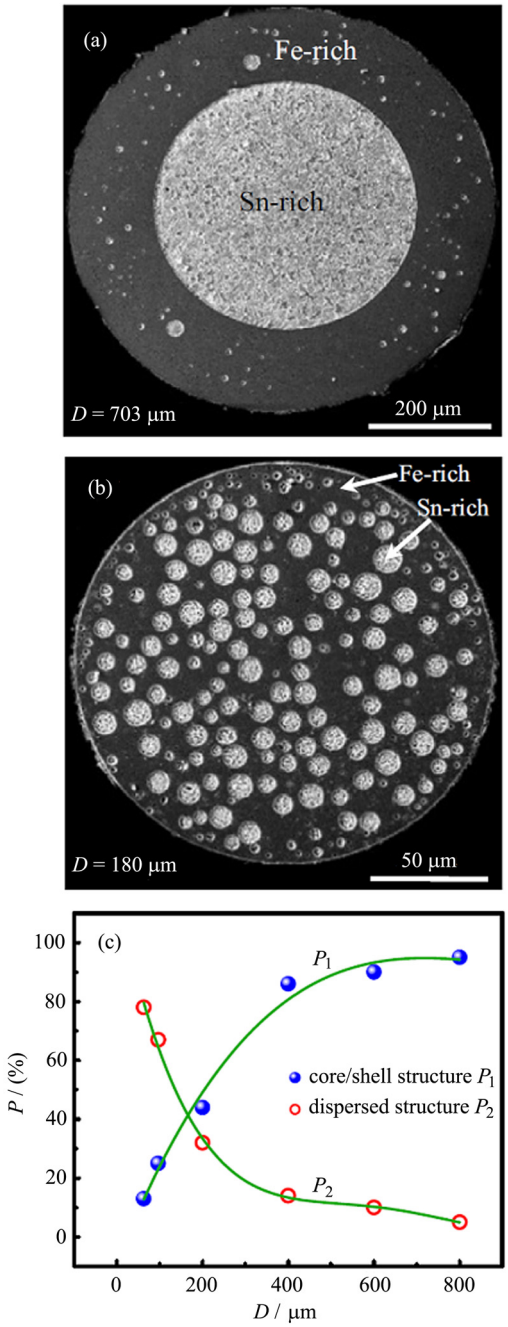

Fig. 3 Two typical microstructures of ternary $Fe_{62}Sn_{34}Ge_4$ immiscible alloy droplets solidified inside drop tube. (a) Two-layer core/shell microstructure at $D = 703\,\mu$m, (b) dispersed microstructure at $D = 180\,\mu$m, and (c) the formation probabilities of core/shell and dispersed microstructures versus alloy droplet diameter

In addition, the dynamic solidification of binary and ternary alloys was also carried out with the introduction of ultrasonic vibration. The published experimental results of Wei's group include the eutectic growth of Sn-Pb[39] and Ag-Cu-Ge alloys[40], peritectic solidification of Sb-Sn[41] and Cu-Sn alloys[42], and monotectic solidification of Al-Cu-Sn alloy[43]. Generally, the ultrasound stimulates nucleation and hinders the bulk undercooling. For most of the tested alloys, the primary phases were remarkably refined by the ultrasound, and the faceted phases have a tendency to grow in a nonfaceted manner at high ultrasonic energy. Spherical eutectic cells of (Sn) + (Pb) and spherical monotectic cells of (Al) + (Sn)+θ (Al_2Cu) formed in ultrasonic field and the volume fraction increases with the ultrasound power. Strong ultrasound facilitates or even completes the peritectic transfor-

mation ($L + \varepsilon \rightarrow \eta$) in $Cu_{30}Sn_{70}$ alloy which occurs only to a very limited extent under static condition.

2 Microgravity Material Research Activities in IMR in the Past Two Years

Nickel-base single crystal superalloys are susceptible to various solidification defects in preparation, which are detrimental to properties[44−46]. Investigations show that gravity plays an important role in alloy solidification process and defect formation[47−59]. However, it is difficult to reveal the gravity effects and study the mechanisms through traditional ground-based solidification experiments. Under microgravity conditions, the effects of gravity on solidification process can be neglected. Therefore, under the financial support of the National Natural Science Foundation of China (No. 51171196), using the microgravity environment produced by a 50 m long drop tube, the dendritic morphologies, characteristics sizes and solute distribution formed under normal gravity and microgravity of binary to quinary Nickel-base single crystal alloys with different contents of W, Ta, Al and Ti elements were comparatively investigated. Besides, Al-Cu alloys and DZ483 nickel-base superalloys were also investigated to explore the effect of microgravity on equiaxial dendrites and the influence of solidification segregation on liquid densities in mushy zone. The results indicate the following conclusions.

Under microgravity condition, the primary dendrite arm spacing of Ni-4.9%Al, Ni-9.6%W and Ni-5.9%Ta binary alloys were all increased, and the microsegregation of the three alloys were more significant. Under normal gravity condition, apparent macrosegregation of solute elements were observed in the three alloys, while, no such tendency could be found under microgravity condition.

Under microgravity condition, the dendrites of Ni-5%Al-8%W, Ni-5%Al-6%Ta, Ni-5%Al-8%W-4%Ti and Ni-5%Al-8%W-4%Ti-3%Ta alloys are more developed, the primary dendrite arm spacing increased, the secondary arms were longer, and developed tertiary dendrites appeared.

Under microgravity condition, the secondary dendrite arm spacing of Ni-5%Al-8%W and Ni-5%Al-8%Ta decreased, while those of Ni-5%Al-8%W-4%Ti and Ni-5%Al-8%W-4%Ti-3%Ta increased.

Under normal gravity condition, along upward growth direction in ternary to quinary alloys, Al contents in primary dendrite arm had tendency to increase, W and Ti contents had tendency to decrease; while under microgravity condition, the change tendency of the three elements were not apparent. No obvious influence of gravity level on Ta content in dendrite arms could be found.

The addition of Ta or Ti into alloys significantly accelerated their solidification processes under normal gravity condition, and increased the difference between the primary dendrite arm spacing formed under the two gravity conditions.

Compared with under normal gravity condition, except the microsegregation of Al was always weaker, those of the other elements could be either stronger or weaker in ternary to quinary alloys under microgravity condition. The addition of Ti into alloys was beneficial to weaken the microsegregation of Al and W, and the addition of Ta into alloys was beneficial to weaken the microsegregation of W, while the segregation of Ti and Ta themselves did not appear to be much different between the two gravity levels.

Research on Al-Cu alloys indicates that the primary and secondary dendrite arm spacing became smaller, and microsegregation became weaker under microgravity condition. Due to smaller density of primary equiaxed dendrites, they floated above the top of epitaxially growing columnar dendrites under the effect of gravity. Under microgravity however, because there was no buoyancy convection, some of the equiaxed dendrites were engulfed by epitaxially growing columnar dendrites. Besides, gravity environment was evidently more conducive to the growth of equiaxed dendrites, and promoted coarsening of equiaxed dendrites and interdendritic eutectic.

Research on mushy zone density of DZ483 alloy indicates that due to different segregation behavior of various alloy elements and precipitation of MC carbides, especially the strong segregation of Ta and Ti in-between dendrites and W in dendrites, the density of liquid in mushy zone inversed. This will arouse thermos-solutal convection under the effect of gravity, and make freckles easier to form. MC carbides precipitate at temperature slightly below the liquidus can retard the quick reduce of liquid density to a certain extent, this supplies an idea to control the precipitation of MC carbides by adjusting C content in alloy so that to avoid the occurrence of freckles.

To summarize the above results, the conclusions can be drawn as follows.

(1) Microgravity environment can enlarge or shrink dendrite arm spacing, and can weaken or enhance microsegregation, depending on the density, content, redistribution behavior of solute elements. Various elements work together, change the density of melt in front of liquid/solid interface, and therefore, change local concentration distribution, which alter the growth speed, solute transportation and supercooling degree there, resulting in the change of dendrite structure, interdendritic structure, precipitate morphology and amount.

(2) Buoyancy convection does not always increase effective diffusion coefficient, it may also decrease effective diffusion coefficient, especially in area among dendrites, which is related with local solute concentration and probably radial temperature gradient.

(3) Due to lighter or heavier respectively, Al and W initiate buoyancy convection and result in macrosegregation. However, no such tendency are observed aroused by Ti and Ta. This may be because they speed up solidification process under normal gravity. Therefore, Al and W are apt to produce channel effect, but Ti and Ta can decrease their segregation.

(4) Under normal gravity, once equiaxial dendrites formed, they will rise above and are repelled by upward growing columnar dendrites if they are lighter. While they will be engulfed by upward growing columnar dendrites and form stray grains if they are heavier.

(5) Density inversion occurs in mushy zone because of solute segregation, which may produce thermo-solutal convection under gravity, and therefore make freckles easier to form. Precipitation of carbides at the temperature slightly below liquidus may suppress the rapid decrease of melt density, which could be applied to avoid the occurrence of freckle.

Besides the above works, under the support of the manned space flight project (No. TGJZ80701-2-RW018), by using the microgravity environment in space, and combining with ground-based comparison experiments, the dendritic morphologies, characteristics sizes as well as solute segregation and defect formation under normal gravity and microgravity of an AlCuMgZn single crystal alloy are planning to comparatively investigated during Tiangong-2 mission. The aim of this work is also to explore the role of gravity in dendrite growth process and solute segregation as well as solidification defect formation. At the present, almost all the ground-based preparation tests and examinations, such as sample and ampoule design, process experiment and optimization, matching experiment together with the multifuctinal space material experiment device and mechanical environmental test, *etc.*, have been finished. It is planed that Tiangong-2 space laboratory will be launched later in 2016. During its flight, an AlCuMgZn single crystal sample encapsulated in quartz ampoule will conduct directional solidification in the multifunctional space material experiment device boarded on it, meanwhile, same experiment under equivalent conditions on the ground will be performed as well to supply a reference object. After the space experiment is finished and the sample is recovered, the samples experimented both in space and on the ground will be comparatively analyzed to get the results.

3 Solidification and Crystal Growth in Space: Materials Science Program in the SJ10-Recoverable Scientific Experiment Satellite

The virtual absence of gravity-dependent phenomena in microgravity allows an in-depth understanding of fundamental events that are normally obscured and therefore are difficult to study quantitatively on Earth[60−61]. Particular interest is that the low-gravity environment aboard spacecraft provides a unique platform to synthesize alloys of semiconductors and metals with homogeneous composition distributions, on both the macroscopic and microscopic scales, due to the much reduced buoyancy-driven convection[60]. Moreover, the easy realization of detached solidification in microgravity suppresses the formation of defects such as dislocations and twins, and thereby the crystallographic perfection is greatly increased[62−63].

Motivated by these facts, the materials science program in the SJ-10 recoverable scientific experiment satellite mainly focuses on the following issues: (i) the growth of large-size semiconductor crystals with uniform composition and low defect density, and high quality metal alloys or composites that cannot be obtained from ground; (ii) understanding how the gravity-driven phenomena affect the crystal growth, and elucidating the site occupation of doping atoms, revealing the liquid/solid interfacial structures, as well as clarifying the microstructure evolution of the metal alloys (or composites) during the solidification process. We hope our program not only provides new sights into the crystal growth mechanism, but also guides the terrestrial crystal preparations.

The materials science program in the SJ-10 recoverable satellite, which is led by Prof. X. W. Zhang from the Institute of Semiconductors, Chinese Academy of Sciences, includes 8 experimental tasks: (i) space growth of GaMnSb diluted magnetic semiconductors, (ii) space synthesis and characterization of high-performance thermoelectric semiconductors, (iii) new generation of infrared semiconductors grown in space, (iv) space growth, numerical simulation and characterization of InGaSb ternary photoelectric crystals, (v) space solidification and defect control of the super alloy single crystals, (vi) interfacial phenomena during the melting of the tin-based alloys, (vii) synthesis of metal matrix composites by self-propagating

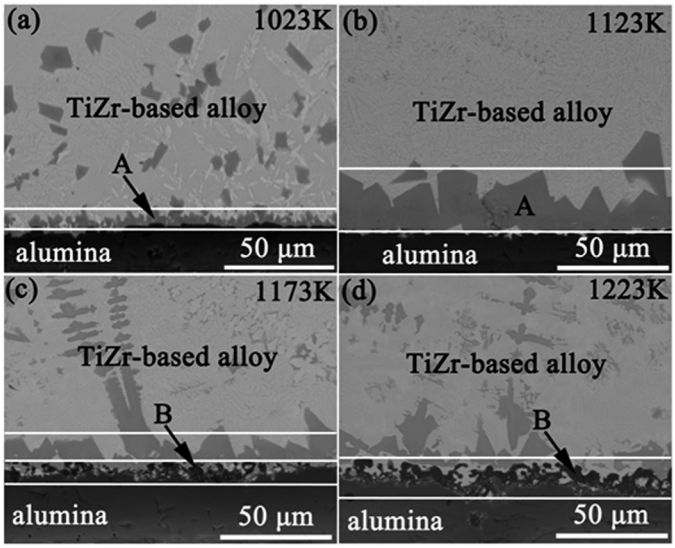

Fig. 4 SEM images at the interfaces of the $Ti_{32.8}Zr_{30.2}Ni_{5.3}Cu_9Be_{22.7}/Al_2O_3$ system synthesized at 1023 K (a), 1123 K (b), 1173 K (c) and 1223 K (d) with saturation time of 60 minutes

reaction under microgravity environment, and (viii) the wettability of molten metal and preparation of metal matrix composites in space[64]. The series of scientific experiments will be carried out successively in the same multiple materials processing furnace with precise controls on the ampoule moving speed and the temperature gradient, and as a result the total load mass can be considerably reduced.

The scientific ampoules have been designed and fabricated under strict quality control procedures. In order to verify their high-safeties, multiple rounds of mechanical tests have been performed under the simulated conditions. Moreover, a large number of terrestrial crystal growth experiments have been carried out using the multiple materials processing furnace to achieve the optimal growth parameters (see, for instance, Figure 4). Now the materials science program in the SJ-10 recoverable satellite enters the critical stage and the final preparations are under way to ensure the success of our experiments.

References

[1] HU L, WANG H P, XIE W J, WEI B. Electrostatic levitation under the single-axis feedback control condition [J]. *Sci. China: Phys. Mech. Astron.*, 2010, **53**: 1438-1444

[2] HU L, WANG H P, LI L H, WEI B. Geometric optimization of electrostatic fields for stable levitation of metallic materials [J]. *Sci. China*: *Technol. Sci.*, 2013, **56**: 53-59

[3] HU L, WANG H P, LI L H, WEI B. Electrostatic levitation of plant seeds and flower buds [J]. *Chin. Phys. Lett.*, 2012, **29**: 064101

[4] LI L H, HU L, YANG S J, WANG W L, WEI B. Thermodynamic properties and solidification kinetics of intermetallic Ni_7Zr_2 alloy investigated by electrostatic levitation technique and theoretical calculations [J]. *J. Appl. Phys.*, 2016, **119**: 035902

[5] HU L, LI L H, YANG S J, WEI B. Thermophysical properties and eutectic growth of electrostatically levitated and substantially undercooled liquid $Zr_{91.2}Si_{8.8}$ alloy [J]. *Chem. Phys. Lett.*, 2015, **621**: 91-95

[6] HONG Z Y, XIE W J, WEI B. Acoustic levitation with self-adaptive flexible reflectors [J]. *Rev. Sci. Instr.*, 2011, **82**: 074904

[7] HONG Z Y, XIE W J, WEI B. Vibration characteristics of acoustically levitated object with rigid and elastic reflectors [J]. *Chin. Phys. Lett.*, 2010, **27**: 014301

[8] GENG D L, XIE W J, YAN N, WEI B. Surface waves on floating liquids induced by ultrasound field [J]. *Appl. Phys. Lett.*, 2013, **102**: 041604

[9] GENG D L, XIE W J, YAN N, WEI B. Vertical vibration and shape oscillation of acoustically levitated water drops [J]. *Appl. Phys. Lett.*, 2014, **105**: 104101

[10] SHEN C L, XIE W J, WEI B. Parametrically excited sectorial oscillation of liquid drops floating in ultrasound [J]. *Phys. Rev.*, 2010, **81**: 046305

[11] SHEN C L, XIE W J, YAN Z L, WEI B. Internal flow of acoustically levitated drops undergoing sectorial oscillations [J]. *Phys. Lett.*: *A*, 2010, **374**: 4045-4048

[12] YAN Z L, XIE W J, WEI B. Vortex flow in acoustically levitated drops [J]. *Phys. Lett.*: *A*, 2011, **375**: 3306-3309

[13] ZHOU K, WANG H P, WEI B. Determining thermophysical properties of undercooled liquid Ti-Al alloy by electromagnetic levitation [J]. *Chem. Phys. Lett.*, 2012, **521**: 52-54

[14] ZHOU K, WANG H P, CHANG J, WEI B. Specific heat measurement of stable and metastable liquid Ti-Al alloys [J]. *Appl. Phys.*: *A* , 2011, **103**: 135-137

[15] ZHOU K, WANG H P, WEI B. Thermophysical properties of substantially undercooled liquid Ti-Al-Nb ternary alloy measured by electromagnetic levitation [J]. *Philos. Magaz. Lett.*, 2013, **93**: 138-141

[16] ZHOU K, WANG H P, CHANG J, WEI B. Surface tension measurement of metastable liquid Ti-Al-Nb alloys [J]. *Appl. Phys.*: *A* , 2011, **105**: 211-214

[17] CHANG J, WANG H P, ZHOU K, WEI B. Surface tension measurement of undercooled liquid Ni-based multicomponent alloys [J]. *Philos. Magaz. Lett.*, 2012, **92**: 428-435

[18] CHANG J, WANG H P, ZHOU K, WEI B. Thermophysical properties and rapid solidification of an undercooled liquid hexabasic Ni-based alloy [J]. *Philos. Magaz. Lett.*, 2013, **93**: 254-263

[19] WANG H P, YANG S J, WEI B. Molecular dynamics prediction of density for metastable liquid noble metals [J]. *Chem. Phys. Lett.*, 2012, **539**: 30-34

[20] WANG H P, WEI B. Positive excess volume of liquid Fe-Cu alloys resulting from liquid structure change [J]. *Phys. Lett.*: *A*, 2010, **374**: 4787-4792

[21] WANG H P, CHANG J, WEI B. Density and related thermophysical properties of metastable liquid Ni-Cu-Fe ternary alloys [J]. *Phys. Lett.*: *A*, 2010, **374**: 2489-2493

[22] LI L H, WANG W L, HU L, WEI B. First-principle calculations of structural, elastic and thermodynamic properties of Fe-B compounds [J]. *Intermetallics*, 2014, **46**: 211-221

[23] ZHAI W, ZHOU K, HU L, WEI B. Determination of the enthalpy of fusion and thermal diffusivity for ternary $Cu_{60-x}Sn_xSb_{40}$ alloys [J]. *J. Chem. Thermodyn.*, 2016, **95**: 159-163

[24] LUO S B, WANG W L, CHANG J, XIA Z C, WEI B.

A comparative study of dendritic growth within undercooled liquid pure Fe and $Fe_{50}Cu_{50}$ alloy [J]. *Acta Mater.*, 2014, **69**: 355-364

[25] XIA Z C, WANG W L, LUO S B, WEI B. Liquid phase separation and rapid dendritic growth of highly undercooled ternary $Fe_{62.5}Cu_{27.5}Sn_{10}$ alloy [J]. *J. Appl. Phys.*, 2015, **117**: 054901

[26] CHANG J, WANG H P, ZHOU K, WEI B. Rapid dendritic growth and solute trapping within undercooled ternary Ni-5%Cu-5%Mo alloy [J]. *Appl. Phys. A* , 2012, **109**: 139-143

[27] CHANG J, WANG H P, WEI B. Rapid Solidification characteristics of highly undercooled liquid Ni-Cu-Mo-Ge quaternary alloy under electromagnetic levitation condition [J]. *Proc. AASRI Int. Confer. Industr. Electron. Appl.*, 2015, **2**: 22-25

[28] WANG W L, QIN H Y, XIA Z C, WEI B. Primary dendrite growth of Ni3Sn intermetallic compound during rapid solidification of undercooled Ni-Sn-Ge alloy [J]. *Chin. Sci. Bull.*, 2012, **57**: 1073-1077

[29] GENG D L, XIE W J, WEI B. Containerless solidification of acoustically levitated Ni-Sn eutectic alloy [J]. *Appl. Phys. A*, 2012, **109**: 239-244

[30] YAN N, GENG D L, HONG Z Y, WEI B. Ultrasonic levitation processing and rapid eutectic solidification of liquid Al-Ge alloys [J]. *J. Alloys Compounds*, 2014, **607**: 258-263

[31] YAN N, GENG D L, HONG Z Y, WEI B. Rapid solidification of acoustically levitated Al-Cu-Si eutectic alloy under laser irradiation [J]. *Chin. Sci. Bull.*, 2011, **56**: 912-918

[32] ZHAI W, WEI B B. Direct nucleation and growth of peritectic phase induced by substantial undercooling condition [J]. *Mater. Lett.*, 2013, **108**: 145-148

[33] LUO S B, WANG W L, XIA Z C, WU Y H, WEI B. Solute redistribution during phase separation of ternary Fe-Cu-Si alloy [J]. *Appl. Phys.*: *A*, 2015, **119**: 1003-1011

[34] ZANG D Y, WANG H P, DAI F P, LANGEVIN D, WEI B. Solidification mechanism transition of liquid Co-Cu-Ni ternary alloy [J]. *Appl. Phys.*: *A*, 2011, **102**: 141-145

[35] WANG W L, LI Z Q, WEI B. Macrosegregation pattern and microstructure feature of ternary Fe-Sn-Si immiscible alloy solidified under free fall condition [J]. *Acta Mater.*, 2011, **59**: 5482-5493

[36] WU Y H, WANG W L, XIA Z C, WEI B. Phase separation and microstructure evolution of ternary Fe-Sn-Ge immiscible alloy under microgravity condition [J]. *Comput. Mater. Sci.*, 2015, **103**: 179-188

[37] YAN N, WANG W L, LUO S B, HU L, WEI B. Correlated process of phase separation and microstructure evolution of ternary Co-Cu-Pb alloy [J]. *Appl. Phys.*: *A*, 2013, **113**: 763-770

[38] YAN N, HONG Z Y, GENG D L, WANG W L, WEI B. Phase separation and structure evolution of ternary Al-Cu-Sn immiscible alloy under ultrasonic levitation condition [J]. *J. Alloys Compounds*, 2012, **544**: 6-12

[39] ZHAI W, HONG Z Y, XIE W J, WEI B. Dynamic solidification of Sn-38.1% Pb eutectic alloy within ultrasonic field [J]. *Chin. Sci. Bull.*, 2011, **56**: 89-95

[40] ZHAI W, LU X Y, WEI B. Microstructural evolution of ternary $Ag_{33}Cu_{42}Ge_{25}$ eutectic alloy inside ultrasonic field [J]. *Progr. Nat. Sci.*, 2014, **24**: 642-648

[41] ZHAI W, WEI B B. Peritectic solidification characteristics of Sb-Sn alloy under ultrasonic vibration [J]. *Mater. Lett.*, 2015, **138**: 1-4

[42] ZHAI W, HONG Z Y, WEN X L, GENG D L, WEI B. Microstructural characteristics and mechanical properties of peritectic Cu-Sn alloy solidified within ultrasonic field [J]. *Mater. Design*, 2015, **72**: 43-50

[43] ZHAI W, LIU H M, WEI B. Liquid phase separation and monotectic structure evolution of ternary $Al_{62.6}Sn_{28.5}Cu_{8.9}$ immiscible alloy within ultrasonic field [J]. *Mater. Lett.*, 2015, **141**: 221-224

[44] WANG Lin, DONG Jianxin, YANG Chunjun, XIE Xishan. Mechanisms for Macro Segregation Freckles and Their Criteria [J]. *Foundry Technol.*, 2007, **28**(5): 585-89 (王玲, 董建新, 杨春军, 谢锡善. 宏观偏析黑斑形成机理及其判据 [J]. 铸造技术, 2007, **28**(5): 585-589)

[45] AL-JARBA K A, FUCHS G E. Effect of carbon additions on the as-cast microstructure and defect formation of a single crystal Ni-based superalloy [J]. *Mat. Sci. Eng. A*, 2004, **373**(1/2): 255-267

[46] BECKERMANN C, GU J P, BOETTINGER W J. Development of a freckle predictor *via* Rayleigh number method for single-crystal nickel-base superalloy castings [J]. *Metall. Mater. Trans. A*, 2000, **31**(10): 2545-2557

[47] SUN Dongke, ZHU Mingfang, YANG Chaorong, PAN Shiyan, DAI Ting. Modelling of dendritic growth in forced and natural convections [J]. *Acta Phys. Sin.*, 2009, **58**: 285-291 (孙东科, 朱鸣芳, 杨朝蓉, 潘诗琰, 戴挺. 强制对流和自然对流作用下枝晶生长的数值模拟 [J]. 物理学报, 2009, **58**: 285-291)

[48] ZHOU B H, JUNG H, MANGELINCK-NOEL N, *et al.* Comparative study of the influence of natural convection on directional solidification of Al-3.5wt% Ni and Al-7wt% Si alloys [J]. *Adv. Space Res.*, 2008, **41**(12): 2112-2117

[49] BANASZEK J, MCFADDEN S, BROWNE D J, STURZ L, ZIMMERMANN G. Natural convection and columnar-to-equiaxed transition prediction in a front-tracking model of alloy solidification [J]. *Metall. Mater. Trans.*: *A*, 2007, **38**(7): 1476-1484

[50] TRIVEDI R, MIYAHARA H, MAZUMDER P, SIMSEK E, TEWARI S N. Directional solidification microstructures in diffusive and convective regimes [J]. *J. Cryst. Growth*, 2001, **222**(1/2): 365-379

[51] JIANG Mingwei, DU Weidong, SONG Changjiang, GAO Yulai, ZHAI Qijie. Effects of specimen dimensions on directional solidification microstructure and interface sta-

bility of Al-4.5%Cu alloy [J]. *Foundry*, 2007, **56**(12): 1307-1309 (蒋明伟, 杜卫东, 宋长江, 高玉来, 翟启杰. 试样尺寸对 Al-4.5%Cu 合金定向凝固组织和界面稳定性的影响 [J]. 铸造, 2007, **56**(12): 1307-1309)

[52] ZHU C S, WANG Z P, GUI J, XIAO R Z. Convection effect on dendritic growth using phase-field method [J]. *China Foundry*, 2010, **7**(1): 52-56

[53] TAN L J, ZABARAS N. Modeling the growth and interaction of multiple dendrites in solidification using a level set method [J]. *J. Comput. Phys.*, 2007, **226**(1): 131-155

[54] YUAN L, LEE P D. Dendritic solidification under natural and forced convection in binary alloys: 2D versus 3D simulation [J]. *Model. Simul. Mater. Sc.*, 2010, **18**(5): 1277-1284

[55] STEINBACH I. Pattern formation in constrained dendritic growth with solutal buoyancy [J]. *Acta Mater.*, 2009, **57**(9): 2640-2645

[56] ASTA M, BECKERMANN C, KARMA A, *et al.* Solidification microstructures and solid-state parallels: Recent developments, future directions [J]. *Acta Mater.*, 2009, **57**(4): 941-971

[57] MA D X, BUHRIG-POLACZEK A. Avoiding grain defects in single crystal components by application of a heat conductor technique [J]. *Int. J. Mater. Res.*, 2009, **100**(8): 1145-1151

[58] YANG X L, NESS D, LEE P D, D'SOUZA N. Simulation of stray grain formation during single crystal seed melt-back and initial withdrawal in the Ni-base superalloy CMSX4 [J]. *Mat. Sci. Eng.*: *A*, 2005, **413**: 571-577

[59] GAO Sifeng, LIU Lin, HU Xiaowu, GE Bingming, ZHANG Jun, FU Hengzhi. Review of freckle defects under directional solidification of nickel-based superalloys [J]. *J. Mat. Sci. Eng.*, 2010, **28**(1): 145-151 (高斯峰, 刘林, 胡小武, 葛丙明, 张军, 傅恒志. 镍基高温合金定向凝固过程中雀斑缺陷研究进展 [J]. 材料科学与工程学报, 2010, **28**(1): 145-151)

[60] STRELOV V I, KURANOVA I P, ZAKHAROV B G, VOLOSHIN A E. Crystallization in space: results and prospects [J]. *Crystallogravity*, 2014, **59**: 781

[61] CHEN N F, ZHONG X R, LIN L Y, *et al.* Comparison of field effect transistor characteristics between space-grown and earth-grown gallium arsenide single crystal substrates [J]. *Appl. Phys. Lett.*, 2001, **78**: 478

[62] DUFFAR T, DUSSERRE P, PICCA F, LACROIX S, GIACOMETTI N. Bridgman growth without crucible contact using the dewetting Phenomenon [J]. *J. Cryst. Growth*, 2000, **211**: 434

[63] HERLACH D M, COCHRANE R F, EGRY I, FECHT H J, GREER A L. Containerless processing in the study of metallic melts and their solidification [J]. *Int. Mater. Rev.*, 1993, **38**: 273

[64] HU W R, ZHAO J F, LONG M, *et al.* Space program SJ-10 of microgravity research [J]. *Microgravity Sci. Tech.*, 2014, **26**: 159